Journal of Mobile Multimedia, Vol. 7, No. 3 (2011) 163–176

A METHOD FOR DISTANCE ESTIMATION USING INTRA-FRAME OPTICAL FLOW WITH AN INTERLACE CAMERA

TSUTOMU TERADA
Graduate School of Engineering, Kobe University
1-1 Rokkodai, Nada Ward, Kobe, Hyogo 657-8501, Japan
tsutomu@eedept.kobe-u.ac.jp

YUHKI SUZUKI
Westunitis, Co., Ltd.
1-1 Rokkodai, Nada Ward, Kobe, Hyogo 657-8501, Japan
yu-suzuki@stu.kobe-u.ac.jp

MASAHIKO TSUKAMOTO
Graduate School of Engineering, Kobe University
1-1 Rokkodai, Nada Ward, Kobe, Hyogo 657-8501, Japan
tuka@kobe-u.ac.jp

Received February 25, 2011
Revised August 29, 2011

Recently, there are many researches on location estimation using optical flow, which is a well-known distance estimation method without any infrastructure. However, since the calculation of optical flow needs high computational power, it cannot adapt to high-speed movement. Therefore, in this paper, we propose *intra-frame optical flow*, which is a new distance estimation method using an interlace camera. It can estimate the high speed moving objects accurately because it uses two successive images with a very short scanning interval extracted from one image captured by an interlace camera. The evaluation result confirmed the effectiveness of our method.

Keywords: Distance estimation, interlace camera

Communicated by: D. Taniar & E. Pardede

1 Introduction

In order to realize location-aware applications such as navigation systems[1, 2], we need a low cost and flexible location estimation method that tracks objects in high-speed movements. There are many location estimation methods using GPS[3], RFID tag[4], visual markers[5], and electric wave intensity[6]. However, GPS gives rough positions and other methods require environmental infrastructures. As examples without using any infrastracture, there are methods using wearable sensors[7] and the optical flow with wearable camera[8]. The former proposed a system that estimates the relative location by a pedometer. However, since it is highly depend on the walking characteristics of human being, it is difficult to be applied to disabled people or robots. The latter estimates the movement by processing an image captured by camera. However, the use of optical flow has problems of estimation errors especially in the case where a camera or an opponent object moves in high speed.

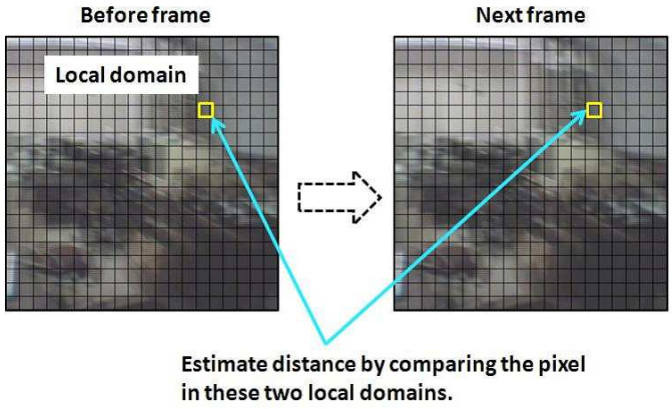

Fig. 1. Calculation of optical flow

In this paper, we propose a new method of estimating the relative distance using intra-flame optical flow by using an interlace camera. Our method estimates the relative position only with a interace camera. Moreover, since our method uses two successive images with a very short scanning interval captured by an interace camera, it can adapt to high speed movements. In addition to this, usually the optical flow explains only the two-dimensional relative position by one camera. For acquiring the three-dimensional relative position, there are several methods using multiple cameras, maultiple markers, and landmarks[9, 10]. State et al. proposed a method using magnetic sensors and landmarks taken by two cameras[9]. Neumann et al. proposed a method measuring three-dimensional location by detecting multiple markers[10]. They need high installation cost that spoil the merit of using optical flow. Therefore, we also propose a simple method to estimate three-dimensional relative position only with an interace camera.

The rest of this paper is organized as follows. Section 2 explains the proposal method in detail, and Section 3 shows our evaluation results. Finally, we summarize the paper in Section 4.

2 Proposed method

The optical flow is a vector that means the distance and the direction of movement for each pixel in successive two images. There are some methods to calculate the optical flow vector. In this paper, we employ the Lucas-Kanade method that is one of the gradient based methods and it is well knows as a method that is lightweight in calculation. The gradient based method calculates the optical flow based on the assumption "the distance of the shade distribution that expresses the feature of a moving object is minute in successive two images." Lucas-Kanade method divides one image into multiple domains as shown in Fig. 1, and it calculates the difference of luminosity and time differentiation of luminosity between the partial domains of a successive frame.

2.1 The problem of optical flow

Supposing the distance estimation by optical flow is performed on software, a system captures images continuously by the camera and estimates the migration distance by comparing two

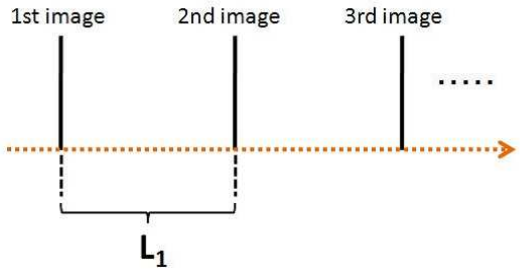

Fig. 2. Calculation interval with progressive camera

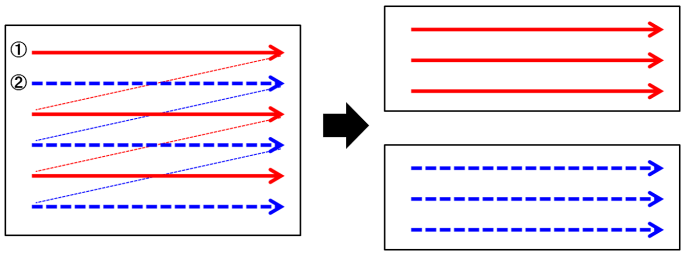

Fig. 3. Characteristic of interlace scan

successive images as shown in the left of Fig. 2. In that case, each processing time L_1 includes the capturing time, the time of storing the image, and the time of distance calculation. At this time, the frequency of picture acquisition is $f_1 = (1/L_1)$. If the computational power of PC or the frame rate of the camera is poor, L_1 becomes longer because the calculation of optical flow requires high computational resource. Thus, in such environment, it is difficult to estimate the migration distance of the object that moves in high-speed.

3 Proposed method

In order to realize a general-purpose location estimation in ubiquitous computing environments, it requires no infrastructure such as markers, and it should support the high-speed object movement. In the proposal method, by using optical flow, it achieves the distance estimation without any infrastructure. Furthermore, by utilizing the feature of interlace camera, which one image consists of two images with a very short scanning interval, we achieve the distance estimation in the case of high-speed movement.

3.1 The Characteristics of interlace camera

When a non-interlace camera takes an image, it starts scanning from the upper left point and moves horizontally to right. Then, it goes on to the next lower horizontal line. All lines are scanned in a progressive way. In case of using an interlace camera, the line scan is done in a similar manner, but firstly only odd lines are scanned and then even lines are done. For example, when the frame rates of camera is 30fps, the frame rates of interlace camera is virtually 60fps if we consider that the odd-line scanning image and even-line scanning image of interlace scan are different images as shown in Fig. 3. We call these images *odd-line scanning image* and *even-line scanning image*.

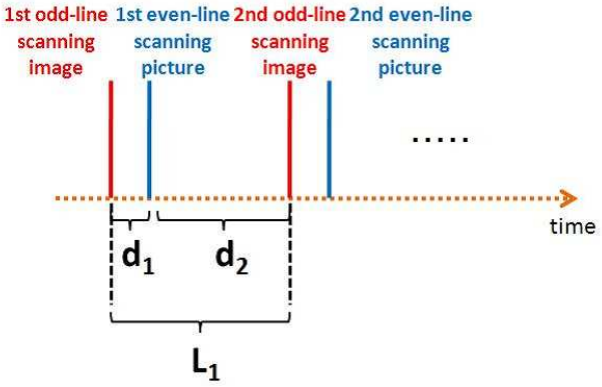

Fig. 4. Calculation interval with interlace camera

Moreover, as shown in Fig. 4, since the interlace camera takes one image from two images with a very short scanning interval d_1, which is much shorter than L_1, the system calculates the optical flow using these two images. At this time, the frequency of distance estimation is virtually $f_p = (1/d_1) = f_1(L_1/d_1)$. Therefore, in the same environment, the accuracy of estimation is the same as that in the case of using the camera that has frequency of d_1, which is L_1/d_1 times faster than that in the conventional method. It clearly means that our method can adapt to high-speed movement of object compared with the conventional method. Moreover, the interlace scan has another merit that the system can perform enough accurate estimation even in the case where the PC or the camera have poor performance in which the capturing interval is too long for using non-interlace camera. This is because d_2 becomes longer in this situation but d_1 is still very short.

3.2 Algorithm

Fig. 5 shows the flow of processing for our proposed method. The detailed processing for each step is shown in the followings:

1. Image capture

   The system captures an image by an interlace camera. We suppose that the camera takes a 640×480 pixels RGB image for simple explanation.

2. Resolution conversion

   It resizes the image into 240×480 pixels using Nearest Neighbor Method. Nearest Neighbor Method is a simple and well used method that allocates the value of nearest pixel to the output pixel[11].

3. Gray scale conversion

   The image converted to gray scale image for simple processing.

4. Division into odd-line scanning image and even-line scanning image

   The system divides the image into the odd-line scanning image and the even-line scanning image.

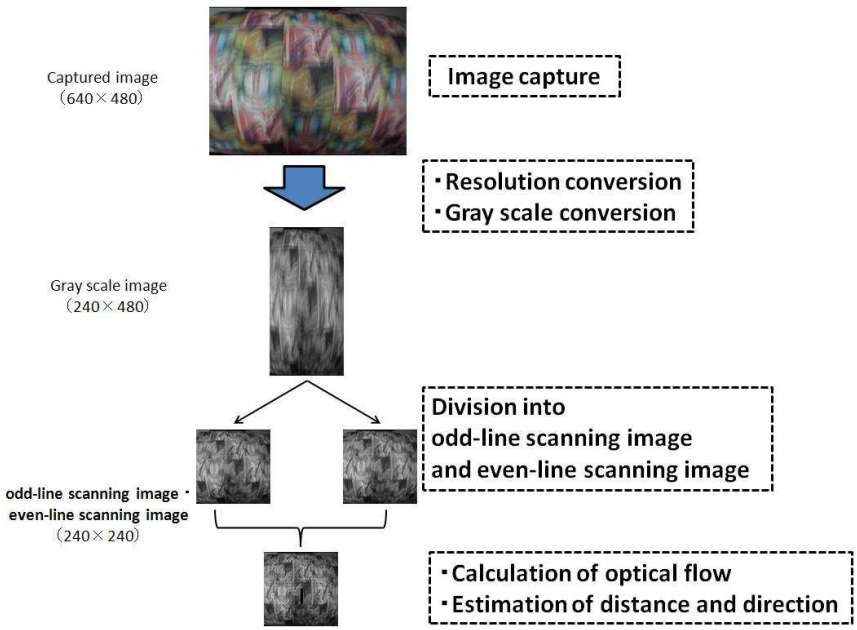

Fig. 5. Flow of processing

5. Calculation of optical flow

   The system calculates the optical flow using the even-line scanning image and the odd-line scanning image by Lucas-Kanade method[12]. In that case, as shown in Fig. 6, each image is divided into 10×10 of local domains, and the system does not use the area of 20 pixels from the edge. The size of local domain is 11×11 pixels, and our method calculates the optical flow using the pixels in each local domain. Furthermore, it accumulates all the estimated optical flow vectors in one frame as the optical flow of the frame.

3.3 Extension to three dimensions

In our assumptions, a camera is attached to airplanes or robots to detect the positions. In this situation, the system can detect the three dimensional position from the horizontal movement, the rotation of camera itself, and the virtical movement. Horizontal movement can be calculated by the optical flow described in the previous sections. Therefore, we propose a method to calculate the remaining two factors.

1. Estimation of virtical motion

   When a camera approaches the ground, the optical flow vector is obtained as shown in Fig. 7 because the ground in a camera becomes large. The system calculates the distance of movement R by measuring the difference between r_2 and r_1, which are the lengths from the central point of a image to the start point and the end point of the vector, respectively. $R = \sum(r_2 - r_1)$, and $R > 0$ when the camera approaches the ground and $R < 0$ when it is getting away from the ground.

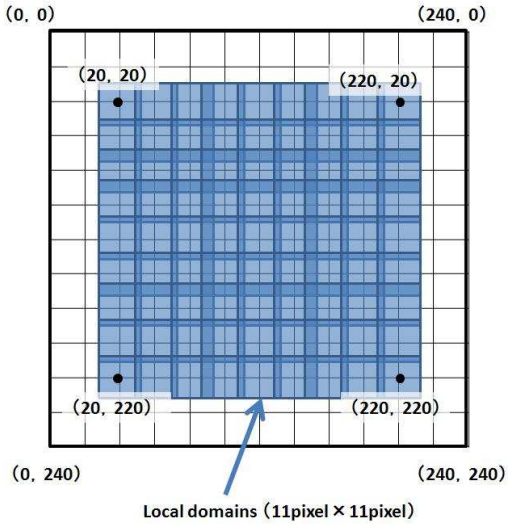

Fig. 6. Local domains

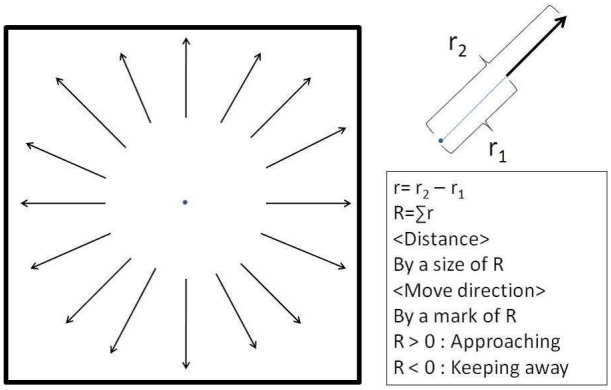

Fig. 7. Optical flow vectors when the camera approaches

2. Estimation of rotation motion

Generally, there are three kinds of rotations as shown in Fig. 8. In this paper, as described above, we suppose only the case where a camera rotates facing to the ground like yaw in the figure. For example, when the camera rotates clockwise, a optical flow vector is obtained as shown in Fig. 9. Therefore, the system calculates the degree of rotation θ by measuring the difference between θ_1 and θ_2, which are the angles from the base point line to the start point and the end point of the vector in polar coordinates, respectively. $\theta = \sum(\theta_1 - \theta_2$, and $\theta > 0$ when the camera rotates clockwise and $\theta < 0$ when it rotates anticlockwise.

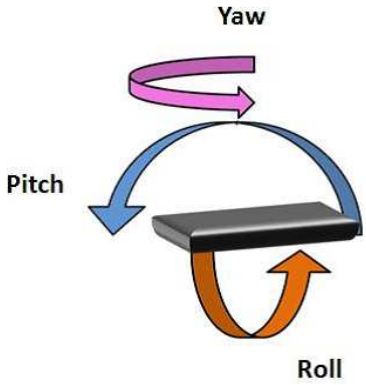

Fig. 8. Three types of rotations

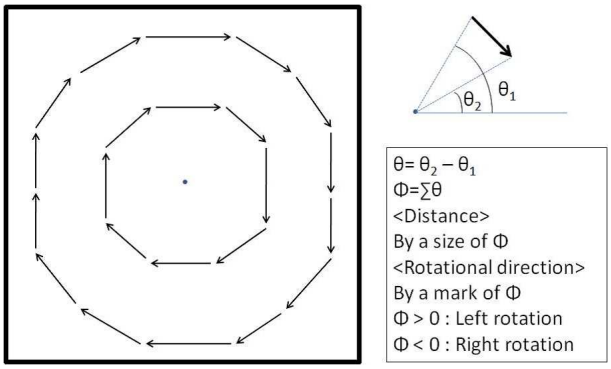

Fig. 9. Optical flow vectors when the camera turns to right

4 Evaluation

4.1 Experiment environment

It will be thought that if we use a high-performance camera and PC, an accuracy of distance estimation improves. However, since a high-performance camera and PC cannot necessarily be used in the case of application, we used camera and PC PC of general performance. As interlace camera, we use The CARD 7RL by RF, Inc., which has 270,000 pixels 1/4-inch color CCD. The resolution of the camera is 680×480 and a captured image is sent to PC via USB. Moreover, CPU of used PC is Athlon(tm) 64 Processor 3500+. 980 MHz and a memory is 960MB.

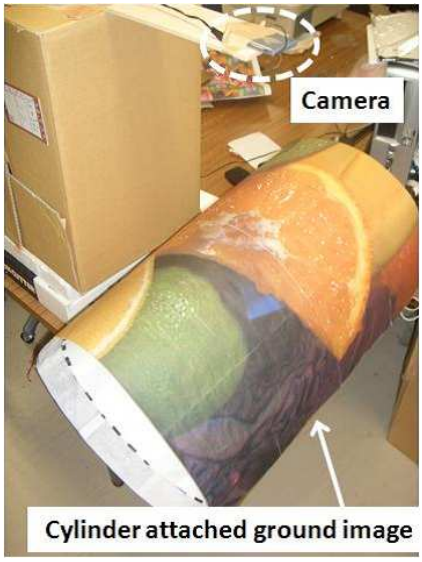

Fig. 10. Experimental setup

4.2 Equipment and a procedure

4.2.1 horizontal direction

Fig. 10 show the experimental apparatus, and Fig. 11 shows the pattern diagrams of experimental apparatus. We install the cylinder that the two background image as shown in Fig. 12 was attached. This image is a standard picture well used by image processing and contained to the image-processing library OpenCV which Intel Corp. exhibits. We compress it 348KB(2446 pixels×2446pixels, 64.71cm×64.71cm). Furthermore, we print to high-quality paper of A4 size by the printer "canon MP 900", and we glued together and used them. The circumference of the cylinder is 127.17cm. The camera is fixed to 33cm distance on a pipe so that the whole background image can fully be photoed with a camera. Note that 1 cm on the cylinder is equivalent to 9.5 pixels on a captured image.

In this experiment environment, we turn the cylinder to the plus direction of y to the camera 3 rounds and take the data of estimated optical flow vector and frame rate. We plot to Graf the movement speed of the cylinder and size of optical flow vector. We perform these operations 90 times, changing revolving speed.

4.2.2 Rotational direction

As shown in Fig. 13, we attach the camera to the rotating equipment, and we stand a background image from a camera at the place of 40cm so that the whole background image can be enough photoed with a camera. At this time, the center of the camera and the center of the background image are coincided. We use the standard picture of Fig. 12, and we compress them into 296KB(3081 pixels×3081 pixels, 81.51cm×81.51cm) by JPEG. Note that 1 cm on the cylinder is equivalent to 5 pixels on a captured image.

We rotate the camera rightward 3 rounds and take the data of estimated optical flow vector and frame rate. Then, we plot to Graf the movement speed of the camera and size of

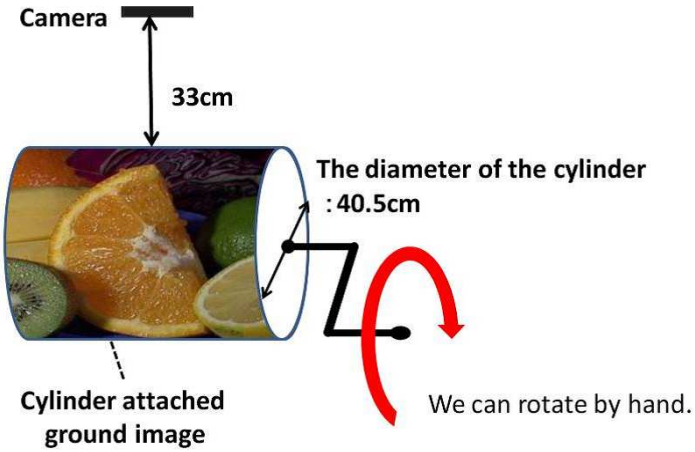

Fig. 11. Setting on experiment (1)

Fig. 12. Ground image used in experiments

optical flow vector. We perform these operations 120 times, changing revolving speed.

4.2.3 Vertical direction

As show in Fig. 14, we attach the camera to a place with a height of 70cm of the cart, and we stand the background image to the place distant 90cm from the camera. At this time, the center of the camera and the center of the background image are coincided. We use the standard picture of Fig. 12, and we compress them into 296KB(3081 pixels×3081 pixels, 81.51cm×81.51cm) by JPEG. Note that when the camera is the furthest from the background image, 1 cm on the cylinder is equivalent to 30 pixels on a captured image, and when the camera is the nearest from the image, 1 cm on the cylinder is equivalent to 240 pixels.

We bring the cart close from the place distant from the background image 90cm to the place of 10cm, and take the data of estimated optical flow vector and frame rate. Then, we plot to Graf the movement speed of the camera and size of optical flow vector. We perform these operations 90 times, changing movmentd speed.

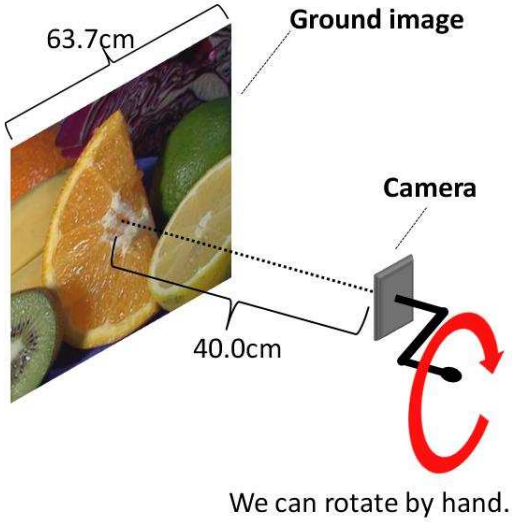

Fig. 13. Setting on experiment (2)

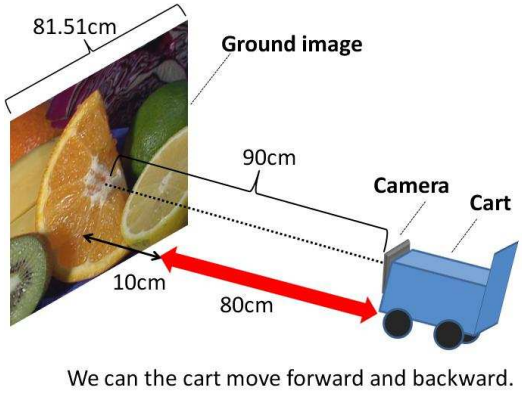

Fig. 14. Setting on experiment (3)

4.3 Comparison method

As the comparison method, we use a non-interlace camera that has the same spec as the camera used in the evaluation for proposal method. In order to arrange conditions, the proposal method and the comparison method are performed within the same program, and these systems take data simultaneously.

4.4 Result

We evaluate by judging that the exact distance estimation is performed, when movement speed and the detection value of an optical flow are in proportionality relation.

4.4.1 horizontal direction

Fig. 15 shows the experimental data. The horizontal axis of the graph shows move speed of the cylinder and the vertical axis show size of estimated optical flow vector. Average of the

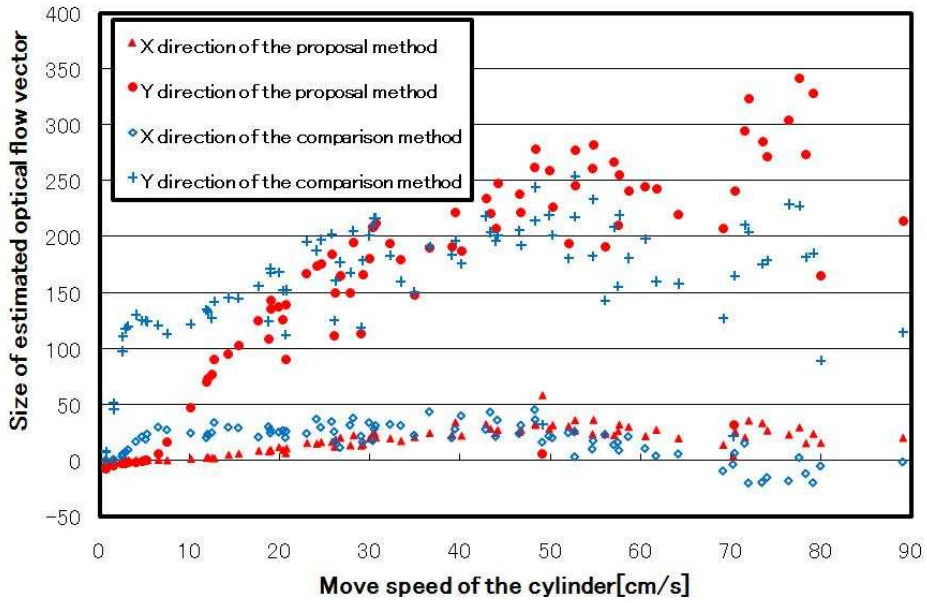

Fig. 15. Result of experiment (1)

frame rate was 5.87 fps, and the illumination intensity of the room was about 1000LUX.

When the cylinder turns in more than a semicircle (about 63.69cm) while the camera captures two images, there is a possibility of leading to an error of measurement, because one kind of two background images are attached to the cylinder(the circumferences is 127.17cm), and the captured two images are same. From an experimental result, it is thought that this error of measurement is not generated because the average of frame rate is about 170.23 [ms] and this phenomenon happens when the movement speed of the cylinder is about 374.14 [cm/s].

By checking the data of the y direction of Fig. 15 which is a direction where the optical flow vector should be detected, we calculate the critical speed that it becomes impossible to perform the exact distance estimation. The critical speed of the proposal method is about 55.0[cm/s] and the critical speed of the comparison method is about 25.0[cm/s]. Therefore, it turns out that the proposal method can support to high-speed movement compared with the comparison method. When checking the data of the x direction which should not be detected ideally, the detection value of the vector is detected although it is a small value compared with a y direction. This is considered to be an error by the experimental apparatus.

4.4.2 Rotational direction

Fig. 16 shows the experimental data. The horizontal axis of the graph shows revolving speed of the camera and the vertical axis show size of estimated optical flow vector. Average of the frame rate was 5.70 fps, and the illumination intensity of the room was about 1000LUX.

When the camera turns around one or more revolutions while the camera captures two images, there is a possibility of leading to an error of measurement. However, in this experi-

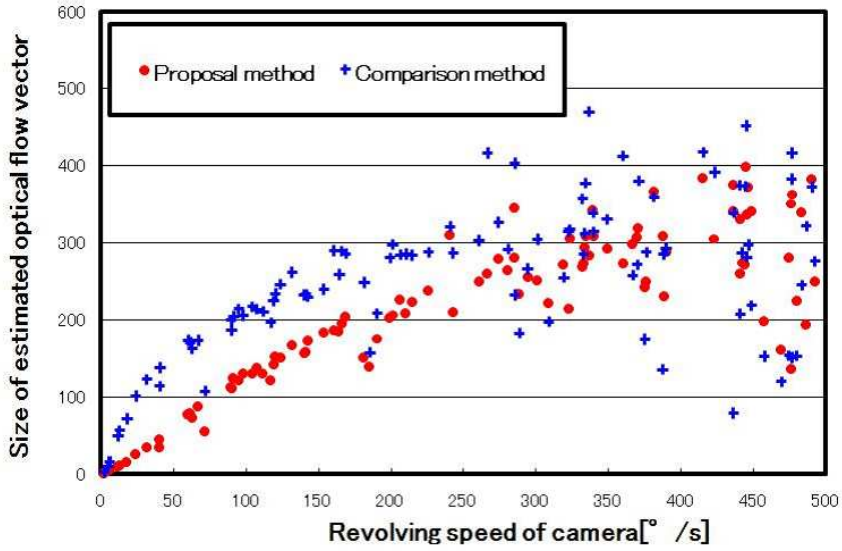

Fig. 16. Result of experiment (2)

mental environment, such a thing has not happened.

By Fig. 16, it turns out that the critical speed of the proposal method is about 370.0[°/s], the critical speed of the comparison method is about 170.0[°/s]. Therefore, it turns out that the proposal method can support to high-speed movement compared with the comparison method. In addition, although the portion as which variation is regarded is in data, it is considered that this is an error by an experimental apparatus.

4.4.3 Vertical direction

Fig. 17 shows the experimental data. The horizontal axis of the graph shows movement speed of the cart and the vertical axis show size of estimated optical flow vector. Average of the frame rate was 5.78 fps, and the illumination intensity of the room was about 1000LUX.

By Fig. 16, it turns out that the critical speed of the proposal method is about 40.0[cm/s], the critical speed of the comparison method is about 20.0[cm/s]. Therefore, it turns out that the proposal method can support to high-speed movement compared with the comparison method. In addition, although the portion as which variation is regarded is in data, it is considered that this is an error by an experimental apparatus.

5 Conclusion

In this paper, we proposed a new distance estimation method using an interlace camera and intra-frame optical flow. Since our system does not use markers, our system can perform general-purpose estimation. Furthermore, since our system estimates relative distance by two successive images with a very short scanning interval captured by a interlace camera, our system adapts the high-speed movement. In addition, we extend the proposal method to the distance estimation method in 3-dimensional space. Our method performs estimation in three-dimensional space by carrying out polar-coordinates conversion of the optical flow

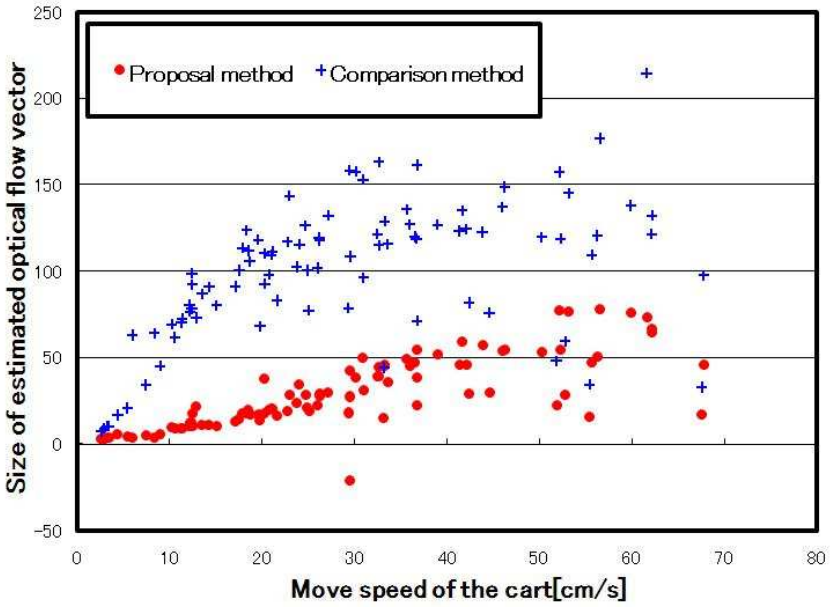

Fig. 17. Result of experiment (3)

obtained from one set of a camera image. Therefore, our method needs not use multiple markers or landmarks, an installation cost is low.

In future, we will apply the proposal method to autonomous control of small helicopter carrying a camera, an air mouse using a camera etc.

References

1. M. Kourogi, N. Sakata, T. Okuma, and T. Kurata: Indoor/Outdoor Pedestrian Navigation with an Embedded GPS/RFID/Self-contained Sensor System, *Proc. of 16th International Conference on Artificial Reality and Telexistence (ICAT2006)*, pp. 1310–1321, 2006.
2. S. Saripalli, J. F. Montgomery, and G. S. Sukhatme: Visually-Guided Landing of an Unmanned Aerial Vehicle, *IEEE Transaction on Robotics and Automation*, vol. 19, No. 3, pp. 371–381, 2003.
3. M. Agrawal, and K. Konolige: Real-time Localization in Outdoor Environments using Stereo Vision and Inexpensive GPS, *Proc. of 18th International Conference on Pattern Recognition (ICPR2006)*, vol. 3, pp. 1063–1068, 2006.
4. D. Hahnel, W. Burgard, D. Fox, K. Fishkin, and M. Philipose: Mapping and Localization with RFID Technology, *Proc. of IEEE International Conference on Robotics and Automation*, vol. 1, pp. 1015–1020, 2004.
5. M. Kalkusch, T. Lidy, M. Knapp, G. Reitmayr, H. Kaufmann, and D. Schmalstieg: Structured Visual Markers for Indoors Pathfinding, *Proc. of The First IEEE International Augmented Reality Toolkit Workshop(ART02)*, 2002.
6. L. Fang, W. Du, and P. Ning: A Beacon-Less Location Discovery Scheme for Wireless Sensor Networks, *Proc. of 24th Annual Joint Conference of the IEEE Computer and Communications Societies*, vol. 1, pp. 161–171, 2005.
7. R. Tenmoku, M. Kanbara, and N. Yokoya: A Wearable Augmented Reality System Using Positioning Infrastructures And A Pedometer, *Proc. of IEEE International Symposium on Wearable ComputersiISWC2003j*, pp. 110–117, 2003.

8. C. Braillon, C. Pradalier, J. L. Crowley, and C. Laugier: Real-time moving obstacle detection using optical flow models, *Proc. of IEEE Intelligent Vehicles Symposium 2006*, pp. 466–471, 2006.
9. A. State, G. Hirota, D. T. Chen, W. F. Garrett, M. A. Livingston: Superior Augmented Reality Registration by Integrating Landmark Tracking and magnetic Tracking, Proc. of SIGGRAPH96, pp. 429–446 i1996j.
10. U. Neumann, S. You, Y. Cho, J. Lee, J. Park,: Augmented Reality Tracking in Natural Environments, Ohmsha and Springer-Verlag, pp. 101–130, i1999).
11. https://www.esrij.com/support/erdas/faq/kiso$_r esample_t ech/kiso_r esample_t ech.jsp$
12. B. Lucas, T. KanadeF An Iterative Image Registration Technique with an Application to Stereo Vision, *Proc. of International Joint Conference on Artificial Intelligence (IJCAI)*, pp. 674–679, 1981.